

Note

The spatial signature of a changing ancient impactor population for Mars

Samuel Holo^{*}, Edwin Kite

Department of Geophysical Sciences, University of Chicago, 5734 S. Ellis Ave., Chicago, IL 60637, United States



ARTICLE INFO

Keywords:

Early Mars
Resurfacing
Impactor populations

ABSTRACT

Ancient solar system processes are recorded by impact crater populations on Mars. We investigated the spatial distribution of Noachian-aged (3.8–4.0 Ga) craters in order to test hypotheses for the shortage of <32 km diameter craters. Using (i) a global database of Mars impact craters and (ii) angular two-point correlation statistics to quantify local to regional crater clustering, we found that degraded craters on low-lying middle-Noachian-highland terrains were subject to spatially-patchy crater obliteration by surface processes, while older, higher-standing craters on the early Noachian highlands remain consistent with being drawn from a spatially uniform distribution. This result supports the hypothesis that the multi-sloped Noachian crater size-frequency distribution results from an early impactor population that changed during the Noachian, rather than from extensive obliteration of craters <32 km in diameter by surface processes such as fluvial erosion, volcanic flooding, and aeolian infilling. The cause of the change in impactor populations remains unknown.

1. Introduction

The Noachian highlands of Mars are heavily-cratered terrain that, in their geology, record ancient (~4 Ga) Mars, the geomorphic evolution of which remains enigmatic (e.g. Irwin et al., 2013). The majority of craters >4 km in diameter on Noachian terrain are degraded (e.g. Craddock and Maxwell, 1993), and several aspects of the Noachian highland landscape can be explained by the interplay of impact cratering and the erosion of crater rims by fluvial erosion (e.g. Forsberg-Taylor et al., 2004, Howard, 2007). Further, examination of latitudinal/elevational trends in crater density and morphometric properties has enabled studies on the history of climatic forcing on crater modification and degradation (e.g. Craddock and Maxwell, 1993; Bouley and Craddock, 2014; Kreslavsky and Head, 2018). While we see abundant evidence for crater degradation by surface processes, our understanding of ancient resurfacing and crater obliteration remains incomplete (Irwin et al., 2013).

The incremental crater size-frequency distribution (CSFD) on the Noachian highlands exhibits a shallow slope in the 4–32 km diameter range, relative to the <4 km and >32 km ranges (Fig. 1). This results in a paucity of craters <~32 km in diameter relative to extrapolation from isochron fits to larger craters (e.g. Irwin et al., 2013; Robbins et al., 2013). This lack of small craters has been observed for decades and is commonly interpreted as the result of diameter-dependent crater obliteration by surface processes such as fluvial erosion, aeolian infilling, volcanic infilling, ejecta infilling, and diffusion (e.g. Öpik, 1966;

Chapman and Jones, 1977; Craddock and Maxwell, 1990; Robbins et al., 2013; Quantin-Nataf et al., 2019). However, surface processes are not the only explanation for the lack of small craters. Specifically, the multi-sloped CSFD on the Noachian highlands is similar to that observed on the Lunar highlands and Mercury's heavily-cratered terrains, while single-sloped CSFD's in the ~1–32 km diameter range are observed in young terrains across these planets (e.g. Barlow, 1988, Strom et al., 2005, Cuk et al., 2010, Fassett et al., 2012, Strom et al., 2015). This suggests that the apparent paucity of craters <32 km in diameter on Noachian terrains could require a distinct inner-solar-system impactor population during the period of heavy bombardment >~3.8 Ga, with a subsequent shift to the modern impactor population and correspondingly single-sloped CSFD (Strom et al., 2005; Fassett et al., 2012; Strom et al., 2015).

These observations beg the questions: did obliteration by surface processes create the shallow-sloped portion of the Noachian CSFD? Can the shape of the Noachian CSFD be attributed to a changing impactor population? Are both required? In this work, we examine the compatibility of the Noachian crater record with each of these scenarios. In particular, we take advantage of statistical advances made by astronomers (e.g. Davis and Peebles, 1983, Bhavsar, 1990, Wall et al., 1993, Landy and Szalay, 1983) to robustly detect clustering of galaxies on the celestial sphere, and we apply their techniques to craters on the Noachian highlands. Assuming that crater-obliteration processes are not spatially uniform (but that impact cratering is), our clustering analysis

^{*} Corresponding author.

E-mail address: holo@uchicago.edu (S. Holo).

<https://doi.org/10.1016/j.icarus.2019.113447>

Received 22 May 2019; Received in revised form 8 August 2019; Accepted 15 September 2019

Available online 18 October 2019

0019-1035/© 2019 Elsevier Inc. All rights reserved.

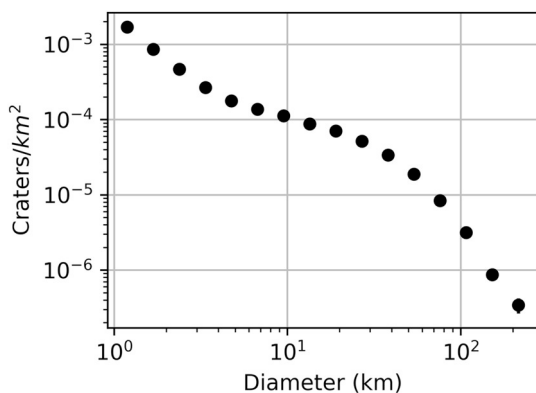


Fig. 1. Incremental crater size-frequency distribution ($2^{0.5}$ -scaled bins, one standard deviation errors smaller than symbols) on the Noachian highlands between 0° N and 30° S latitude (Robbins et al., 2013).

serves as a means of detecting crater-obliteration on ancient geologic surfaces.

2. Geologic datasets and context

To investigate clustering of craters and resurfacing on Noachian highland terrains, we used two global datasets. The first is a global database of crater latitudes, longitudes, diameters, and degradation states (Robbins and Hynek, 2012). The second is a global geologic map of Mars (Tanaka et al., 2014). In this map, the Noachian highlands are divided into three main units (Fig. 2): the early-Noachian highlands (eNh) that were mapped as heavily-cratered, high-standing, rugged, high-relief terrain; the middle-Noachian highlands (mNh) that were mapped as low-lying, often visibly layered, relatively smooth surfaces that make up most of the observable Noachian highlands; and the late-Noachian highlands (lNh) that were mapped as basin fill at topographic minima in the mNh/lNh (Irwin et al., 2013; Tanaka et al., 2014). The eNh unit retains a crater population >32 km in diameter that is near saturation (Irwin et al., 2013), but the mNh and lNh retain lower crater densities for diameters >16 km due to Noachian-era, gravity-dependent burial of large craters by some combination of volcanic, aeolian, and fluvial surface processes (Irwin et al., 2013). Further, the distribution of mapped geomorphic surfaces with distinct modification styles/processes (e.g. debris-mantled escarpments, regolith pediments, depositional plains, and sloping aggradational surfaces) on the Noachian highlands was shown to be variable on $\sim 10^\circ$ angular scales (~ 600 km) (Cawley and Irwin, 2018). The observed spatial non-uniformity of Noachian surface processes motivates use of clustering as a detection of Noachian crater obliteration by erosion/burial.

Integration of these two datasets allowed us to restrict the global Robbins database (Robbins and Hynek, 2012) to craters lying on the eNh and mNh units in the Tanaka et al. (2014) map (Fig. 2). Further, we

restricted our dataset to craters ≥ 4 km in diameter to avoid potential database completeness issues (Stuart Robbins – personal communication) and to craters ≤ 32 km in diameter to avoid incorrectly assigning units to larger craters (many >32 km diameter craters with centers on the mNh or lNh unit can be unambiguously assigned to older units via cross-cutting relationships; see Irwin et al., 2013). Finally, we restricted our dataset to latitudes -30° N to 0° N to avoid potentially confusing signals from post-Noachian high-latitude modification (e.g. Kreslavsky and Head, 2018) and from the extensive resurfacing in Arabia Terra (Hynek and Phillips 2001). We did not restrict our dataset by longitude (Fig. 2).

3. Methods

With our integrated dataset, we quantified crater clustering using the angular two-point correlation function, which has been typically used to quantify clustering of galaxies and test cosmological models (see Wall and Jenkins, 2012). The angular two-point correlation function, $w(\theta)$, is defined in terms of the incremental probability, dP , of finding two craters with separation θ in a solid angle element, $d\Omega$:

$$dP = \bar{R}[1 + w(\theta)]d\Omega$$

where \bar{R} is the probability of finding two points with separation θ in a randomly distributed dataset with the same mean density as our actual data. Thus, $w(\theta)$ can be thought of as a fractional enhancement (or depletion) factor of pairwise distances at a particular scale, relative to that expected for random points from a spatially-uniform distribution. Because $w(\theta)$ is estimated numerically by generating a random catalog of points (with no diameter information) and comparing the pairwise distance distribution to that found in our dataset (see Appendix A), it is easy to incorporate the effects of geologic masking (i.e. by irregular count area geometry from mapped units in Tanaka et al., 2014) by applying the same masking to said random catalog.

To detect clustering on a particular angular scale, one must do more than just estimate $w(\theta)$ for a number of angular separation bins. In particular, $w(\theta)$ can be enhanced on small scales due to longer-wavelength density variations (see Bhavsar, 1990; Wall et al., 1993; Wall and Jenkins, 2012). Thus, the canonical method is to search for increasing $w(\theta)$ with decreasing angular scales by fitting a power-law to $w(\theta)$ and estimating the power-law slope in log-log space (Bhavsar, 1990; Wall et al., 1993; Wall and Jenkins, 2012). Note: we are fitting a power-law function within a limited domain, not a probability distribution subject to normalization constraints, so ordinary least squares regression in log-log space is appropriate. To assess the uncertainty in the slope estimate, one cannot assume any particular distribution structure to the errors, as they are both non-normal and correlated (e.g. Wall and Jenkins, 2012). However, the uncertainty is readily estimated by performing the computation many times, each time generating a new random catalog, and computing pairwise distance from a bootstrapped (resampled with replacement) version of the original dataset each time (Bhavsar, 1990). Examination of the histogram of slope values obtained

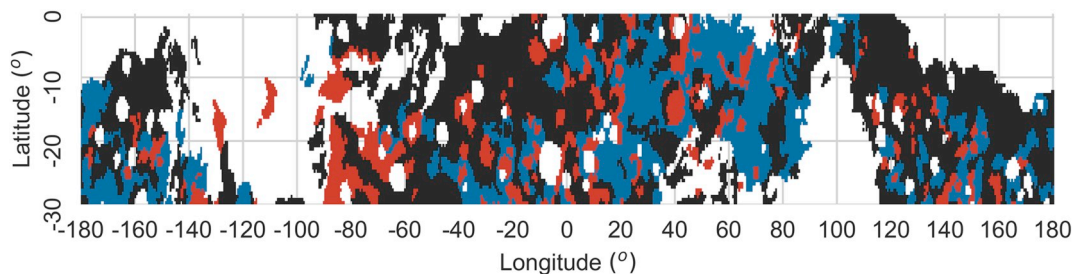


Fig. 2. $0.5^\circ \times 0.5^\circ$ resolution grid of latitudes and longitudes in our study area, colored by geologic unit from Tanaka et al. (2014): blue areas correspond to the eNh, black areas to the mNh, and red areas to the lNh. Areas not colored represent post-Noachian materials or small Noachian massif units (Tanaka et al., 2014). (For interpretation of the references to colour in this figure legend, the reader is referred to the web version of this article.)

allows one to determine how frequently the slope is <0 and thus, how confident one is that a clustering signal exists (Wall et al., 1993). In this study, we demonstrate the application of this procedure to craters of different sizes, degradation states, and maximum ages to gain insight into resurfacing in the early and middle Noachian highlands.

4. Clustering of Noachian craters

We binned our crater database by diameter (factor-of-2 width bins), geologic unit (we exclude the late Noachian highlands unit due to large uncertainties in calculated two-point correlations), and degradation state (grouping qualitatively determined preservation states 1&2 and 3&4 as “degraded” and “fresh,” respectively). These qualitative determined preservation states are described in more detail in Robbins and Hynek (2012). For each of these groupings, we estimated the angular two-point correlation function in 10 logarithmically-spaced separation bins between 2° and 30° (Fig. 3, also see the Appendix A). Further, we computed 500 bootstrapped estimates of the corresponding power-law slope to determine to what extent craters on each unit, in a particular diameter range, experienced local to regional variations in crater obliteration (Fig. 4).

We found that morphologically fresh craters have correlation power-law slopes that are consistent with 0, regardless of diameter or geologic unit (Fig. 4). This indicates that, as expected, fresh craters are consistent with being randomly drawn from a spatially uniform distribution on the surveyed scales. On the early Noachian highlands unit (‘eNh’ in Tanaka et al., 2014), we found that degraded craters between 4 and 8 km in diameter show statistically significant clustering (Fig. 4), but that no such signal exists for degraded craters >8 km in diameter (Fig. 4). On the middle Noachian highlands unit (‘mNh’ in Tanaka et al., 2014), we found statistically significant clustering in each of the 4–8, 8–16, and 16–32 km diameter bins of degraded craters.

5. Implications for ancient resurfacing and impactor populations

As stated above, we assume that impacts are spatially uniform but that crater-obliteration processes are not. Thus, from the geologic context of heavily degraded craters (e.g. Craddock and Maxwell, 1993), one may expect the observed clustering for degraded craters 4–8 km in diameter on both mNh and eNh terrains to be the result of spatially-

patchy crater obliteration by surface processes. While we favor this explanation, we note that the reference random catalogs for our two-point correlation function estimates contain no diameter/mutual occlusion information. As a result, it is at least in principle possible for clustering of craters to occur from obliteration by larger craters, or, “cookie-cutting” (Michael et al., 2012; Christian Riedel, personal communication). However, the cookie-cutting effect should increase in efficiency with overall crater density. Thus, we can attribute clustering of 8–32 km diameter degraded craters on the mNh unit to spatially-patchy obliteration and resurfacing processes. Our reasoning is as follows: if this clustering on the mNh unit did arise from cookie-cutting, then one would expect a clustering signal to be present for the 8–16 km bin on the eNh unit, which has a similar number of craters (~ 1000) as the 16–32 km bin on the larger mNh unit (and thus similar statistical power of the test), but greater overall density. However, this clustering signal is not observed. In addition, secondary craters may produce clustering signals (e.g. Riggs et al., 2015), but most secondary craters are too small to significantly affect our sampled populations (Robbins and Hynek, 2014).

We found that resurfacing of the mNh unit was spatially patchy on local-to-regional scales, not just on planetary length scales. This result is consistent with the study of Cawley and Irwin (2018). Further, because degraded craters >8 km in diameter on the eNh unit are consistent with being drawn randomly from a spatially uniform distribution, we conclude that Noachian resurfacing processes on the local topographic highs comprising the unit (Irwin et al., 2013; Tanaka et al., 2014) were weak (relative to those on the mNh) and did not fully bury large craters. That the eNh has (a) craters in the 8–32 km that are consistent with being drawn randomly from a spatially uniform distribution and (b) a shallower sloping 8–32 km CSFD than does the mNh (Irwin et al., 2013), indicates that diameter-dependent obliteration alone cannot explain the shallow-sloped portion of the Noachian CSFD. Instead (or in addition), the data requires that the impactor SFD changed during the Noachian, perhaps due to planet migration or a late heavy bombardment (e.g. Barlow, 1988; Strom et al., 2005; Strom et al., 2015).

6. Discussion

We made use of the angular two-point correlation function as a means of detecting clustering of craters on a range of pre-specified scales. Other methods have been used to detect crater clustering, but

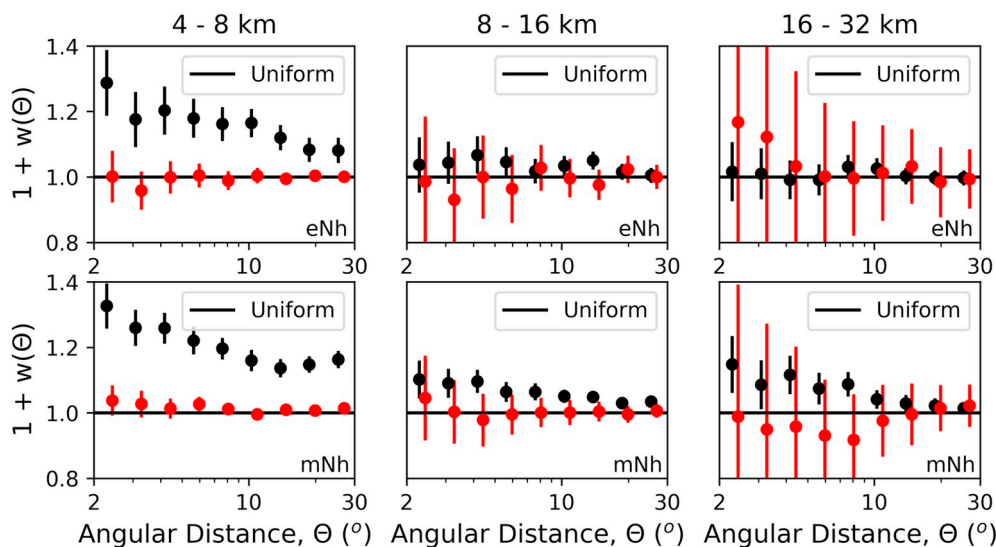


Fig. 3. Results from computation of the angular two-point correlation function for different diameter bins and geologic units (eNh-top row, mNh- bottom row). Fresh craters are shown in red, and degraded craters are shown in black. Error bars are one standard deviation, but recall that errors are non-normal and correlated. (For interpretation of the references to colour in this figure legend, the reader is referred to the web version of this article.)

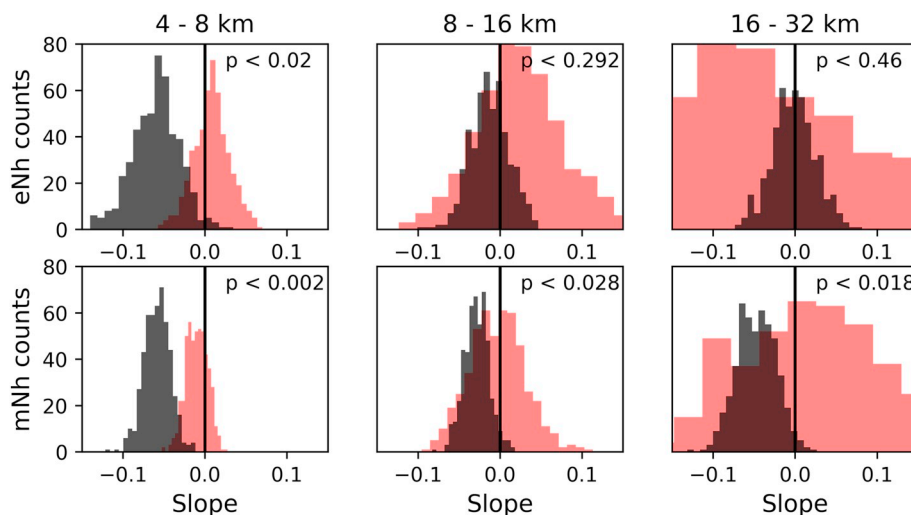


Fig. 4. Histograms of bootstrapped best-fit power-law slopes for the angular two-point correlation function for different diameter bins and geologic units. Fresh craters are shown in red, and degraded craters are shown in black. All fresh craters are consistent with being drawn randomly from a spatially uniform distribution. p = significance level for degraded craters. (For interpretation of the references to colour in this figure legend, the reader is referred to the web version of this article.)

these methods rely on nearest-neighbor statistics (e.g. [Squyres et al., 1997](#); [Kreslavsky, 2007](#); [Michael et al., 2012](#); [Kirchoff, 2017](#)). Nearest-neighbor statistics detect clustering only on the scale of nearest-neighbors, which is itself dependent on point density (and can thus complicate comparisons of different crater diameter ranges). In contrast, the two-point correlation function preserves information from all scales, and our detection procedure is performed on a pre-specified range of scales (e.g. [Wall and Jenkins, 2012](#); [Riggs et al., 2015](#)). Finally, the two-point correlation function is rigorously statistically defined, with well-understood errors and estimators (e.g. [Wall and Jenkins, 2012](#)), while nearest neighbor statistics are not (e.g. [Riggs et al., 2015](#)).

We combined mapped stratigraphic relationships, crater degradation classifications, and robust detection of crater clustering (via correlation function power-law slope determination) to draw conclusions about local to regional resurfacing on the Noachian highlands. In principle, because the angular two-point correlation function provides amplitude information (not just a binary detection output), it can provide higher-order information than what was utilized in this study. This has been done extensively by astronomers, who are able to explicitly model the two-point correlation function from the basic physics of the systems observed (e.g. [Blake and Wall, 2002](#)). However, the two-point correlation function does not preserve phase information and is less sensitive than power-spectrum analysis for larger angular scales (e.g. [Wall and Jenkins, 2012](#)). Thus, other metrics of clustering could be useful in unraveling global-scale resurfacing.

In our analysis, we assumed that detection of clustering served as a detection of obliteration by spatially-patchy surface processes (or even “cookie-cutting” of small craters by large impact craters). It is feasible that clustering could be observed due to real anisotropies in Mars’ impactor flux ([Le Feuvre and Wicczorek, 2008](#)). However, on the measured scales of 2° to 30° , density variations are expected to be small ([Le Feuvre and Wicczorek, 2008](#)). This is corroborated by the fact that fresh craters in the Noachian highlands are all consistent with being drawn randomly from a spatially uniform distribution ([Fig. 4](#)). In addition, surface processes can in principle obliterate craters uniformly (e.g. resurfacing by planetary-scale impacts), but these are not likely relevant to Noachian era resurfacing ([Irwin et al., 2013](#); [Cawley and Irwin, 2018](#)).

Our work was partly motivated by recent studies that use the observed paucity of small craters on the Noachian highlands to infer the maximum depth of burial/erosion in various areas ([Robbins et al., 2013](#); [Quantin-Nataf et al., 2019](#)). While our study does not invalidate their overall approach, it does invalidate the assumption that crater

production functions (and thus the shape of fit isochrons) do not change in time. Further, our study provides evidence for a changing impactor population for Mars, but does not retrieve exactly how that population has changed as a function of time. As a result, revised determination of the maximum depth of burial on different terrains in the Noachian highlands is beyond the scope of this paper. We note that it is possible, in principle, that estimates of maximum burial/erosion depth that incorporate a changing production function will not significantly differ from previous estimates, but that estimates of typical burial/erosion depth (which should more strongly influence regional clustering) change drastically.

While our study supports the hypothesis that the population of objects bombarding pre-3.8 Ga Mars was different than the population of objects currently bombarding Mars post-3.8 Ga, the cause of this shift remains unknown. The hypothesis that giant planets migrated around 3.8 Ga (e.g. [Strom et al., 2005](#)) has been supplanted by the hypothesis that major shifts in the orbits of the giant planets occurred >4.45 Ga ([Morbidelli et al., 2018](#); [Nesvorný et al., 2018](#)). This is probably too old to explain our data. An incomplete list of processes that may have contributed to changes in the size-frequency distribution of Mars-crossing objects includes: collisional grinding within the asteroid belt ([Bottke et al., 2005](#); [Bottke and Morbidelli, 2017](#)); tidal disruption of a Vesta-sized object ([Cuk et al., 2010](#)); or early size-agnostic sweep-up by Mars of an extension of the asteroid belt ([Cuk and Nesvorný, 2018](#)).

7. Conclusions

Integration of a global database of craters ([Robbins and Hynek, 2012](#)) with globally mapped geologic units ([Tanaka et al., 2014](#)) enabled us to examine the first-order stratigraphic (i.e. geologic age) control on clustering (as measured by the angular two-point correlation function) of degraded Noachian highland craters. We found that low-lying, middle Noachian highland terrains experienced spatially varying rates of resurfacing and burial that produced clustering of >8 km diameter craters on 2° – 30° angular scales. However, early Noachian craters are consistent with being drawn randomly from a spatially uniform distribution, implying shallow burial/erosion on the high-standing eNh unit (relative to the mNh). Our result supports the hypothesis that the multi-sloped CSFD on the Noachian highlands requires changes in crater production (e.g. [Strom et al., 2005](#); [Strom et al., 2015](#)), rather than spatially-patchy destruction of craters alone (e.g. [Öpik, 1966](#); [Chapman and Jones, 1977](#); [Craddock and Maxwell, 1990](#); [Robbins et al., 2013](#); [Quantin-Nataf et al., 2019](#)).

Acknowledgments

We thank David Mayer and Stuart Robbins for helpful discussions.

We thank Caleb Fassett and Ross Irwin for thoughtful reviews. We acknowledge funding from NASA grants (NNX16AG55G, NNX16AJ38G).

Appendix A. Estimating the angular two-point correlation function

We described $w(\theta)$ as an “enhancement factor” of pairwise distances relative to that expected for random points from a spatially-uniform distribution. This interpretation leads to an intuitive method for estimating $w(\theta)$ (Blake and Wall, 2002). First, one generates a random uniformly-distributed set of n_r points and masks it to the same area as the data (which in our case is the geologic unit under investigation). One then computes DD, the counts of pairwise distances (in bins of separation) of craters within our database. One also computes RR, the counts of pairwise distances of craters in the randomly generated catalog. Finally, one computes:

$$w(\theta) = \frac{n_r(n_r - 1)}{n_D(n_D - 1)} \frac{DD}{RR} - 1$$

where n_D is the number of craters in our data set. This intuitively ratios the probability distribution of measured pairwise distances to that expected in a random catalog. Landy and Szalay (1983) demonstrated that an improved estimator, which involves calculating DR (pairwise distances between points in the data set and in the random catalog), can significantly reduce bias:

$$w(\theta) = \frac{n_r(n_r - 1)}{n_D(n_D - 1)} \frac{DD}{RR} - 2 \frac{DR}{RR} \left(\frac{n_r - 1}{n_D} \right) + 1.$$

Thus, we use the Landy and Szalay (1983) estimator throughout our study.

References

- Barlow, N., 1988. Crater size-frequency distributions and a revised Martian relative chronology. *Icarus* 75, 285–305. [https://doi.org/10.1016/0019-1035\(88\)90006-1](https://doi.org/10.1016/0019-1035(88)90006-1).
- Bhavsar, S.P., 1990. Bootstrap, data permuting and extreme value distributions – getting the most out of small samples. In: Jashek, C., Murtagh, F. (Eds.), *Errors, Bias and Uncertainty in Astronomy*. Cambridge University Press, p. 107.
- Blake, C., Wall, J., 2002. Measurement of the angular correlation function of radio galaxies from the NRAO VLA sky survey. *Mon. Not. R. Astron. Soc.* 329, L37–L41. <https://doi.org/10.1046/j.1365-8711.2002.05163.x>.
- Botke, W.F., Morbidelli, A., 2017. Using the main asteroid belt to constrain planetesimal and planet formation. In: Elkins-Tanton, L., Weiss, B. (Eds.), *Planetesimal: Early Differentiation and Consequences for Planets*. Cambridge University press, pp. 38–67.
- Botke, W.F., Durda, D.D., Nesvorný, D., Jedicke, R., Morbidelli, A., Volkrouhlicky, D., Levison, H., 2005. The fossilized size distribution of the main asteroid belt. *Icarus* 175 (1), 111–140. <https://doi.org/10.1016/j.icarus.2004.10.026>.
- Bouley, S., Craddock, R.A., 2014. Age dates of valley network drainage basins and subbasins within Sabae and Arabia Terra, Mars. *Journal of Geophysical Research: Planets* 119, 1302–1310. <https://doi.org/10.1002/2013JE004571>.
- Cawley, J.C., Irwin, R.P., 2018. Evolution of escarpments, pediments, and plains in the Noachian Highlands of Mars. *Journal of Geophysical Research: Planets* 123, 3167–3187. <https://doi.org/10.1029/2018JE005681>.
- Chapman, C.R., Jones, K.L., 1977. Cratering and obliteration history of Mars. *Annu. Rev. Earth Planet. Sci.* 5, 515–538. <https://doi.org/10.1146/annurev.ea.05.050177.002503>.
- Craddock, R.A., Maxwell, T.A., 1990. Resurfacing of the Martian Highlands in the Amenthes and Tyrrhena region. *J. Geophys. Res.* 95, 14265–14278. <https://doi.org/10.1029/JB095IB09p14265>.
- Craddock, R.A., Maxwell, T.A., 1993. Geomorphic evolution of the Martian highlands through ancient fluvial processes. *Journal of Geophysical Research: Planets* 98, 3453–3468. <https://doi.org/10.1029/92JE02508>.
- Cuk, M., Nesvorný, D., 2018. Planetary chaos and the (in)stability of the Hungaria asteroids. *Icarus* 304, 9–13. <https://doi.org/10.1016/j.icarus.2017.04.015>.
- Cuk, M., Gladman, B.J., Stewart, S.T., 2010. Constraints on the source of lunar cataclysm impactors. *Icarus* 207 (2), 590–594. <https://doi.org/10.1016/j.icarus.2009.12.013>.
- Davis, M., Peebles, P.J.E., 1983. A survey of galaxy redshifts. V - the two-point position and velocity correlations. *Astrophys. J.* 267, 465. <https://doi.org/10.1086/160884>.
- Fassett, C.I., Head, J.W., Kadish, S.J., Mazarico, E., Neumann, G.A., Smith, D.E., Zuber, M.T., 2012. Lunar impact basins: stratigraphy, sequence and ages from superposed impact crater populations measured from Lunar Orbiter Laser Altimeter (LOLA) data: crater statistics of lunar impact basins. *Journal of Geophysical Research: Planets* 117. <https://doi.org/10.1029/2011JE003951>.
- Forsberg-Taylor, N.K., Howard, A.D., Craddock, R.A., 2004. Crater degradation in the Martian highlands: morphometric analysis of the Sinus Sabaeus region and simulation modeling suggested fluvial processes. *J. Geophys. Res.* 109 <https://doi.org/10.1029/2004JE002242>.
- Howard, A.D., 2007. Simulating the development of Martian highland landscapes through the interaction of impact cratering, fluvial erosion, and variable hydrologic forcing. *Geomorphology* 91, 332–363. <https://doi.org/10.1016/j.geomorph.2007.04.017>.
- Hynek, B.M., Phillips, R.J., 2001. Evidence for extensive denudation of the Martian highlands. *Geology*, v. 29, 407–410.
- Irwin, R.P., Tanaka, K.L., Robbins, S.J., 2013. Distribution of Early, Middle, and Late Noachian cratered surfaces in the Martian highlands: implications for resurfacing events and processes: Martian Highland cratered surfaces. *Journal of Geophysical Research: Planets* 118, 278–291. <https://doi.org/10.1002/jgre.20053>.
- Kirchoff, M.R., 2017. Can spatial statistics help decipher impact crater saturation? *Meteorit. Planet. Sci.* 53, 874–890. <https://doi.org/10.1111/maps.13014>.
- Kreslavsky, M.A., 2007. Statistical characterization of spatial distribution of impact craters: implications to present-day cratering rate on Mars. In: *International Conference on Mars, 7th, Pasadena, California*, p. 3325.
- Kreslavsky, M.A., Head, J.W., 2018. Mars climate history: insights from impact crater wall slope statistics. *Geophys. Res. Lett.* 45, 1751–1758. <https://doi.org/10.1002/2017GL075663>.
- Landy, S.D., Szalay, A.S., 1983. Bias and variance of angular correlation functions. *Astrophys. J.* 412 (1), 64–71. <https://doi.org/10.1086/172900>.
- Le Feuvre, M., Wieczorek, M.A., 2008. Nonuniform cratering of the terrestrial planets. *Icarus* 197 (1), 291–306.
- Michael, G.G., Platz, T., Kneissl, T., Schmedemann, N., 2012. Planetary surface dating from crater size–frequency distribution measurements: spatial randomness and clustering. *Icarus* 218, 169–177. <https://doi.org/10.1016/j.icarus.2011.11.033>.
- Morbidelli, A., Nesvorný, D., Laurenz, V., Marchi, S., Rubie, D.C., Elkins-Tanton, L., Wieczorek, M., Jacobson, S., 2018. The timeline of the lunar bombardment: revisited. *Icarus* 305, 262–276. <https://doi.org/10.1016/j.icarus.2017.12.046>.
- Nesvorný, D., Volkrouhlicky, D., Botke, W.F., Levison, H.F., 2018. Evidence for very early migration of the solar system planets from the Patroclus-Menoetius binary Jupiter Trojan. *Nature Astronomy* 2, 878–882. <https://doi.org/10.1038/s41550-018-0564-3>.
- Öpik, E.J., 1966. The Martian surface. *Science* 153, 255–265. <https://doi.org/10.1126/science.153.3733.255>.
- Quantin-Nataf, C., Craddock, R.A., Dubuffet, F., Lozac’h, L., Martinot, M., 2019. Decline of crater obliteration rates during early martian history. *Icarus* 317, 427–433. <https://doi.org/10.1016/j.icarus.2018.08.005>.
- Riggs, J.D., Robbins, S.J., Kirchoff, M.R., Bierhaus, E.B., Weaver, B.P., 2015. *Understanding Spatial Statistics for Purposes of Identifying Non-primary and Saturated Impact Crater Populations: Workshop on Issues in Crater Studies and the Dating of Planetary Surfaces*, Laurel, Maryland, p. 9050.
- Robbins, S.J., Hynek, B.M., 2012. A new global database of Mars impact craters ≥ 1 km: 1. Database creation, properties, and parameters: Mars crater database-construction. *Journal of Geophysical Research: Planets* 117. <https://doi.org/10.1029/2011JE003966> p. n/a-n/a.
- Robbins, S.J., Hynek, B.M., 2014. The secondary crater population of Mars. *Earth Planet. Sci. Lett.* 400, 66–76. <https://doi.org/10.1016/j.epsl.2014.05.005>.
- Robbins, S.J., Hynek, B.M., Lillis, R.J., Botke, W.F., 2013. Large impact crater histories of Mars: the effect of different model crater age techniques. *Icarus* 225, 173–184. <https://doi.org/10.1016/j.icarus.2013.03.019>.
- Squires, S., Howell, C., Liu, M., Lissauer, J., 1997. Investigation of crater “saturation” using spatial statistics. *Icarus* 125, 67–82. <https://doi.org/10.1006/icar.1996.5560>.
- Strom, R.G., Malhotra, R., Ito, T., Yoshida, F., Kring, D.A., 2005. The origin of planetary impactors in the inner solar system. *Science* 309, 1847–1850. <https://doi.org/10.1126/science.1113544>.

- Strom, R.G., Malhotra, R., Xiao, Z.-Y., Ito, T., Yoshida, F., Ostrach, L.R., 2015. The inner solar system cratering record and the evolution of impactor populations. *Res. Astron. Astrophys.* 15, 407–434. <https://doi.org/10.1088/1674-4527/15/3/009>.
- Tanaka, K.L., Robbins, S.J., Fortezzo, C.M., Skinner, J.A., Hare, T.M., 2014. The digital global geologic map of Mars: chronostratigraphic ages, topographic and crater morphologic characteristics, and updated resurfacing history. *Planetary and Space Science* 95, 11–24.
- Wall, J.V., Jenkins, C.R., 2012. *Practical Statistics for Astronomers*, 353. Cambridge University Press.
- Wall, J.V., Rixon, G.T., Benn, C.R., 1993. The nature of mJy radio sources. In: Chincarini, G.L., Iovino, A., Maccacaro, T., Maccagni, D. (Eds.), *ASP Conference Series 51: Observational Cosmology*, p. 576.